Photosynthetic assimilation of CO_2 regulates TOR activity

Manuel J. Mallén-Ponce[a], María Esther Pérez-Pérez[a], and José L. Crespo[a,1]

[a]Instituto de Bioquímica Vegetal y Fotosíntesis, Consejo Superior de Investigaciones Científicas–Universidad de Sevilla, Sevilla 41092, Spain

Edited by Michael Hall, Biozentrum, Universitat Basel, Basel, Switzerland; received August 18, 2021; accepted November 29, 2021

The target of rapamycin (TOR) kinase is a master regulator that integrates nutrient signals to promote cell growth in all eukaryotes. It is well established that amino acids and glucose are major regulators of TOR signaling in yeast and metazoan, but whether and how TOR responds to carbon availability in photosynthetic organisms is less understood. In this study, we showed that photosynthetic assimilation of CO_2 by the Calvin–Benson–Bassham (CBB) cycle regulates TOR activity in the model single-celled microalga *Chlamydomonas reinhardtii*. Stimulation of CO_2 fixation boosted TOR activity, whereas inhibition of the CBB cycle and photosynthesis down-regulated TOR. We uncovered a tight link between TOR activity and the endogenous level of a set of amino acids including Ala, Glu, Gln, Leu, and Val through the modulation of CO_2 fixation and the use of amino acid synthesis inhibitors. Moreover, the finding that the *Chlamydomonas* starch-deficient mutant *sta6* displayed disproportionate TOR activity and high levels of most amino acids, particularly Gln, further connected carbon assimilation and amino acids to TOR signaling. Thus, our results showed that CO_2 fixation regulates TOR signaling, likely through the synthesis of key amino acids.

TOR kinase | CO_2 | amino acids | *Chlamydomonas*

The target of rapamycin (TOR) kinase is a fundamental regulator of cell growth and metabolism that integrates nutrient and energy signals to the cell growth machinery (1, 2). TOR associates to other proteins to constitute two functionally and architecturally distinct complexes, termed TOR complexes 1 and 2 (TORC1 and TORC2) (3). The core components of TORC1 include the TOR kinase, Raptor/Kog1 and LST8, whereas TORC2 is composed of TOR, LST8, Sin1/Avo1, and Rictor/Avo3. Like TOR itself, TORC1 and TORC2 are highly conserved in eukaryotes, although TORC2-specific components have not been identified in the green lineage (Viridiplantae).

TOR promotes cell growth in response to the availability of nutrients, activating anabolism and inhibiting catabolism under favorable conditions. Amino acids are main activators of TORC1 signaling in yeast and metazoans, although activation of this pathway in multicellular organisms requires additional input from growth factors (4, 5). In mammals, amino acid abundance is mainly signaled to mTORC1 via the small GTPases RAGs and RHEB and the lysosomal Ragulator complex, while amino acid signaling to TOR is partially conserved in yeast (4, 6). It is currently unknown how many different amino acids are sensed by TORC1 in yeast and mammals, but leucine and arginine are key regulators of mTORC1 activity, and yeast TORC1 responds preferentially to glutamine (4).

TORC1 is structurally and functionally conserved in plants. In *Arabidopsis thaliana*, TORC1 promotes cell growth by regulating fundamental processes, including ribosome biogenesis, transcription, cell expansion, autophagy, metabolism, and nutrient assimilation (7–9). However, upstream regulators of yeast and mammalian TORC1 such as RAGs and RHEB are not conserved in plants, suggesting that different regulatory mechanisms may operate in these organisms. Plant TOR integrates hormone and stress signals, but the underlying mechanisms are poorly understood. The plant hormones auxin and ABA have been identified as positive and negative regulators, respectively, of TOR signaling in *Arabidopsis* (10, 11).

Energy and nutrients are also key regulators of TOR activity in plants. An original study performed in *Arabidopsis* seedlings demonstrated that exogenous glucose activates TOR kinase activity through glycolysis-mitochondria–mediated energy and metabolic relays (12). Neither hormones nor amino acids can substitute for glucose, suggesting that different inputs may act on plant TOR (12). Mounting evidence indicates that amino acid availability modulates TOR activity in plants. Inhibition of branched chain amino acid biosynthesis by genetic or chemical approaches led to TOR inhibition (13, 14), whereas addition of glutamine or isoleucine to leaf discs from *Arabidopsis* stimulates TOR activity (15). In plants, nitrogen is taken up by roots, and studies performed in TOR-overexpressing seedlings correlated root elongation with TOR function under excess nitrate, suggesting that nitrogen is an important nutrient for TOR signaling (16). Supporting this hypothesis, it has been shown that nitrate, ammonium, and glutamine promote TOR activity via activation of the small GTPase ROP2 (17).

TORC1 components are widely conserved in algal genomes, including freshwater and marine species (18, 19). Studies performed in the model green alga *Chlamydomonas reinhardtii* (hereafter *Chlamydomonas*) provided new insights into TOR signaling in photosynthetic eukaryotes (20). Biochemical evidence revealed the presence of *Chlamydomonas* TOR in a high-molecular-mass complex that associates with microsomal

PLANT BIOLOGY

Significance

Photosynthetic organisms are responsible for the incorporation of inorganic carbon in the biosphere through a fundamental process known as carbon fixation. This reaction allows the reduction of inorganic carbon, mostly atmospheric CO_2, to organic compounds such as carbohydrates and amino acids. Despite the biological relevance of carbon fixation in nature, how photosynthetic cells sense carbon availability remains poorly understood. Using the model microalga *Chlamydomonas reinhardtii*, we found that the photosynthetic assimilation of CO_2 regulates the activity of the target of rapamycin (TOR) kinase, a master regulator of cell growth and nutrient sensor widely conserved in all eukaryotes. Our study revealed that inorganic carbon fixation and photosynthesis regulate TOR activity, likely through the synthesis of central amino acids in carbon metabolism.

Author contributions: M.J.M.-P., M.E.P.-P., and J.L.C. designed research; M.J.M.-P. and M.E.P.-P. performed research; M.J.M.-P., M.E.P.-P., and J.L.C. analyzed data; and J.L.C. wrote the paper.

The authors declare no competing interest.

This article is a PNAS Direct Submission.

This open access article is distributed under Creative Commons Attribution-NonCommercial-NoDerivatives License 4.0 (CC BY-NC-ND).

[1]To whom correspondence may be addressed. Email: crespo@ibvf.csic.es.

This article contains supporting information online at http://www.pnas.org/lookup/suppl/doi:10.1073/pnas.2115261119/-/DCSupplemental

Published January 7, 2022.

membranes (21). The sensitivity of *Chlamydomonas* to rapamycin has been exploited to dissect TOR signaling in this alga (22). Chemical inhibition of *Chlamydomonas* TORC1 with rapamycin blocks translation (23), induces the synthesis and storage of triacylglycerol (24), and triggers autophagy (25). Transcriptomic and metabolomic studies of *Chlamydomonas* cells treated with rapamycin uncovered TOR as a central regulator of primary metabolism (26, 27). Moreover, quantitative phosphoproteomic analysis following TOR inhibition identified proteins involved in translation, carotenoid biosynthesis, autophagy, and cell signaling (28, 29).

Despite recent progress on the study of TOR signaling in algae, little is known about upstream regulation of this pathway by nutrients and the underlying mechanisms. The similar response of TOR inhibition and nitrogen starvation suggested that this nutrient might regulate TOR signaling in *Chlamydomonas* (22, 24, 25, 27, 30). The TOR kinase has also been connected to inositol polyphosphate metabolism in *Chlamydomonas*, but the precise role of these molecules in TOR signaling is currently unknown (31). A recent study demonstrated that phosphorus availability regulates TOR activity via LST8 in *Chlamydomonas*. Phosphorus starvation results in a sharp decrease in LST8 abundance and down-regulation of TOR activity (32). The transcription factor PSR1, a global regulator of the phosphorus starvation response in *Chlamydomonas* (33), has been linked to the control of TOR signaling, as neither LST8 level nor TOR activity is properly regulated in PSR1-defective cells (32).

Photosynthetic organisms are able to fix inorganic carbon species like CO_2 to more reduced organic forms, a fundamental process that sustains life on Earth. This reaction is driven by the Calvin-Benson-Bassham (CBB) cycle in the chloroplast of plant and algal cells. Although nutrients such as nitrogen, phosphorus, sulfur, amino acids, and glucose have been shown to regulate TOR in different organisms, it is currently unknown whether this signaling pathway responds to inorganic carbon. In this study, we aimed to investigate whether carbon availability regulates TOR signaling using *Chlamydomonas* as model system. Our results demonstrated that the carbon source is a main regulator of TOR activity. We found that the photosynthetic assimilation of CO_2 efficiently activates TOR, probably through the synthesis of central amino acids.

Results

The Carbon Source Modulates TOR Activity. Given the fundamental role of TOR in coupling nutrient availability to cell growth, we investigated whether the carbon source regulates TOR in *Chlamydomonas*. To this aim, we monitored TOR activity in wild-type cells with atmospheric CO_2 as the sole carbon source (high saline medium, HSM) or using acetate as an additional carbon source [Tris-acetate-phosphate (TAP) medium], which sustains robust growth and biomass productivity in *Chlamydomonas* (ref. 34; Fig. 1*A*). The analysis of RPS6 phosphorylation, an established readout of TOR activity in *Chlamydomonas* (32), revealed a twofold increase in TOR activity in TAP-grown cells (Fig. 1*B*), which is consistent with a previous report showing stimulation of TOR activity under mixotrophic conditions in *Chlamydomonas* (30). The abundance of TOR and LST8 proteins was similar in cells grown either with acetate or atmospheric CO_2 (Fig. 1*B*), indicating that the carbon source might influence TOR activity without altering the level of TORC1 proteins.

Amino acids are main regulators of TOR signaling (4, 5), and a significant portion of assimilated carbon is invested in the synthesis of amino acids in *Chlamydomonas* (34). Thus, to understand why TAP-grown cells displayed higher TOR activity compared to HSM-grown cells, we analyzed the concentration of all amino acids in both conditions. The total amino acid content was around 40% higher in cells using acetate as additional carbon source (*SI Appendix*, Fig. S1*A*), and the level of eight amino acids increased significantly (Fig. 1*C*). This subset of up-regulated amino acids included Glu, Gln, Ala, Val, Leu, Met, Gly, and Pro, some of which (Ala, Leu, Glu, Gln) are among the most abundant amino acids in *Chlamydomonas* (*SI Appendix*, Fig. S1*B*). Taken together, these results showed that the carbon source controls TOR activity in *Chlamydomonas* and pinpoint amino acids as potential TOR regulators.

CO_2 Fixation Promotes TOR Activity. To investigate the link between TOR and carbon assimilation in *Chlamydomonas*, we analyzed the effect of HCO_3^- on RPS6 phosphorylation under autotrophic growth conditions. In aquatic systems, microalgae like *Chlamydomonas* actively transport and efficiently use HCO_3^- as the carbon source for photosynthesis (ref. 35; Fig. 2*A*). Accordingly, it is well established that the addition of HCO_3^- to *Chlamydomonas* cells potently augments photosynthesis (ref. 36; Fig. 2*B*). In this study, we found that HCO_3^- boosted RPS6 phosphorylation within 30 min, indicating that the assimilation of HCO_3^- triggers TOR activity in *Chlamydomonas* (Fig. 2*C*). The impact of HCO_3^- on TOR activity mirrored the stimulation of photosynthesis as both RPS6 phosphorylation and O_2 production gradually decreased following the 30-min HCO_3^- boost (Fig. 2 *B* and *C*). We also analyzed whether HCO_3^- might change the abundance of TOR and LST8 proteins, but no significant effect was detected (Fig. 2*C*). To demonstrate that TOR mediates the increased phosphorylation of RPS6 in response to HCO_3^-, we examined RPS6 phosphorylation upon HCO_3^- addition in rapamycin-treated cells. Indeed, inhibition of TOR by rapamycin fully prevented the HCO_3^--induced phosphorylation of RPS6 (Fig. 2*D*).

We next investigated the mechanism by which HCO_3^- promotes TOR activity in *Chlamydomonas*. For its assimilation, HCO_3^- must be converted to CO_2 through the carbonic anhydrase CAH3 localized in the thylakoid lumen, and then rubisco catalyzes the formation of 3-phosphoglycerate (3PG) from ribulose-1,5-bisphosphate (RuBP) and CO_2, a key reaction in the CBB cycle (ref. 34; Fig. 2*A*). To study the possible effect of disrupting CO_2 fixation on TOR, we used glycolaldehyde (GLA), a specific inhibitor of phosphoribulokinase (PRK) activity that interrupts the CBB cycle and inactivates photosynthesis (37). We indeed confirmed that GLA blocks PSII activity in our experimental setup within 30 to 60 min (*SI Appendix*, Fig. S2). GLA treatment led to a strong decrease of RPS6 phosphorylation that was detectable within 2 h following GLA addition (Fig. 2*E*). Moreover, we found that the inhibition of the CBB cycle by GLA abolished the HCO_3^--mediated up-regulation of TOR activity (Fig. 2*F*), indicating that disruption of CO_2 fixation inhibits TOR activity in *Chlamydomonas*.

Photosynthetic carbon assimilation constitutes a major source of intermediates for the synthesis of amino acids. We thus analyzed whether HCO_3^--induced stimulation of photosynthesis might change the amino acid content in *Chlamydomonas*. Excluding Ser and Gly, the level of all amino acids increased within 30 min of HCO_3^- addition (Fig. 2*G*). Some amino acids (Val, Leu, Ile, Thr, Pro, Met, Phe, Tyr) remained high, while others (Ala, Glu, Gln, Cys, Asp, Asn, Lys, His, Arg, Trp) gradually decreased in the time course of the experiment. Among the transiently up-regulated amino acids, Ala, Glu, Gln, Asp, and Asn displayed a similar trend to TOR activity, peaking at 30 min after HCO_3^- addition. Moreover, Ala and Glu were the amino acids most highly induced by HCO_3^- at 30 min (Fig. 2*G*). We also studied the effect of GLA on the amino acid content in *Chlamydomonas*. In contrast to HCO_3^-, inhibition of CO_2 fixation by GLA caused a progressive decline of most amino acids (Fig. 2*H*). The negative effect of GLA on the amino acid content and TOR activity was evident after 2 to 4

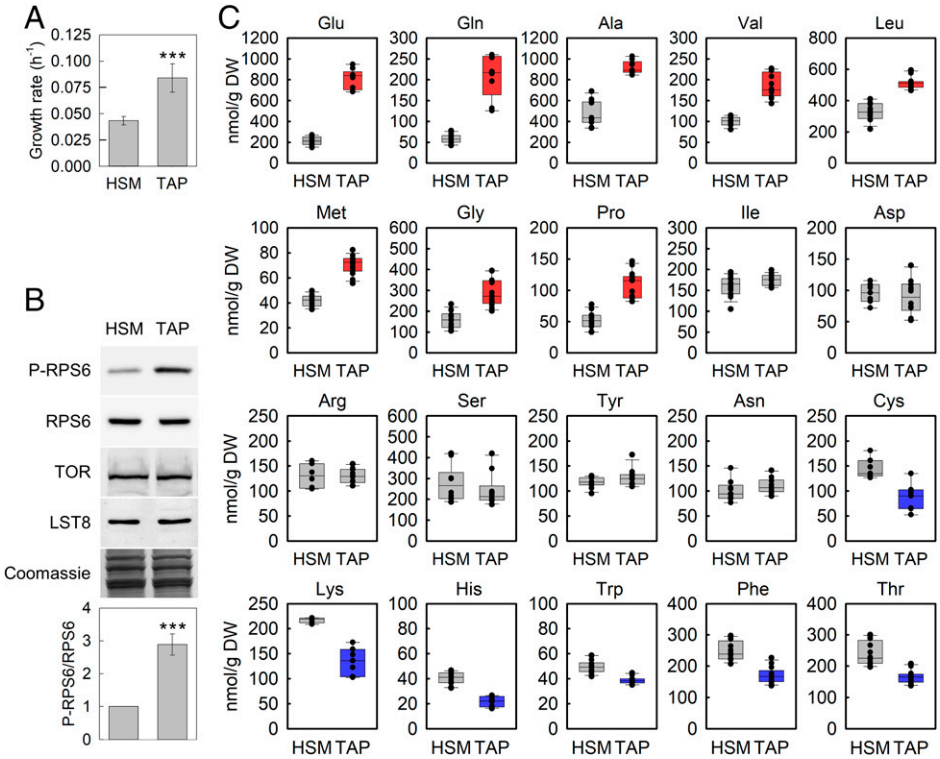

Fig. 1. Carbon source modulates TOR activity in *Chlamydomonas*. (*A*) Growth rate of wild-type 4A+ *Chlamydomonas* cells under autotrophic (HSM) or mixotrophic (TAP) conditions. Growth rate is expressed in h^{-1}, and it was calculated as the increase in cell number during a time period (see *Materials and Methods*). Five biological replicates were analyzed for each condition. (*B*) Immunoblot analysis of phosphorylated RPS6 (P-RPS6), RPS6, TOR, and LST8 proteins in cells growing exponentially in HSM or TAP medium. TOR activity was determined as the ratio of phosphorylated to total RPS6 protein from three biological replicates (a. u., arbitrary units). Coomassie brilliant blue–stained gels were used as protein loading control. (*C*) Amino acid content of *Chlamydomonas* in HSM or TAP medium. Amino acids up-regulated and down-regulated in the presence of acetate (TAP) are shown in red and blue, respectively. Amino acids with no significant change in both media are shown in gray. Each condition included at least eight biological replicates. Error bars represent SD of the mean values. Asterisks represent significant differences according to two-tailed Student's *t* test, ***$P < 0.001$. DW, dry weight.

h since the absolute levels of amino acids at the 1-h time point might still be sufficient to activate TOR, despite a reduction in the relative amount (Fig. 2 *E* and *H*). Actually, the level of some amino acids that might be important for TOR activation such as Gln, Leu, and Val were not decreased after 1 h GLA treatment (Fig. 2*H*). Gln was the only amino acid that remained high in GLA-treated cells, probably because of a decrease in the C/N ratio upon photosynthesis inhibition and the availability of NH_4^+ under these conditions (*SI Appendix*, Fig. S2). These results revealed a tight link between TOR activity and the endogenous level of some amino acids including Ala, Glu, Gln, Leu, and Val in response to the stimulation or inhibition of CO_2 fixation.

Inhibition of Photosynthesis Down-Regulates TOR Activity. Photosynthesis provides ATP and NADPH required for carbon fixation. Based on the regulatory role that CO_2 fixation plays on TOR activity (Fig. 2), we speculated that the disruption of photosynthesis might disturb TOR signaling in *Chlamydomonas*. To test this hypothesis, we monitored TOR activity in air-grown cells subjected to darkness or treated with 3-(3,4-dichlorophenyl)-1,1-dimethylurea (DCMU), an inhibitor of photosynthetic electron transport at PSII level. Our results showed that the inhibition of photosynthesis by darkness or DCMU (*SI Appendix*, Fig. S2) led to a gradual and pronounced decrease of TOR activity (Fig. 3 *A* and *B*). To characterize the regulation of TOR by light, we analyzed the effect of a dark-to-light transition on TOR activity. Interestingly, reillumination of dark-adapted cells resulted in a fast and strong reactivation of TOR (Fig. 3*C*). Moreover, we found that inhibition of CO_2 fixation by GLA fully prevented the reactivation of TOR by light (Fig. 3*C*), further supporting the regulation of TOR by carbon fixation.

We also determined the amino acid content in *Chlamydomonas* cells subjected to darkness or treated with DCMU. Two clusters of amino acids with similar patterns were detected under both conditions. About half of the amino acids declined, following a similar trend to TOR activity, while the other half increased in response to photosynthesis inhibition (Fig. 3*D*). The subset of down-regulated amino acids included Ala, Glu, Gln, Leu, and Val, whose levels were also found to correlate with TOR activity under different carbon sources (Fig. 1) and in response to the stimulation or inhibition of CO_2 fixation (Fig. 2).

The Abundance of Intracellular Amino Acids Regulates TOR Activity. We aimed to establish a direct role of amino acids in the control of TOR signaling by carbon fixation. Given the inability of *Chlamydomonas* cells to transport amino acids other than Arg (38), in order to show a direct link between intracellular amino acids and TOR, we blocked the synthesis of central amino acids. For this purpose, we treated *Chlamydomonas* cells with sulfometuron methyl (SMM), an inhibitor of acetolactate synthase that catalyzes the first common step in the biosynthesis of Leu and Val (ref. 39; Fig. 4*A*), and aminooxyacetate (AOA), which blocks Ala formation by inhibiting alanine aminotransferase (ref. 40; Fig. 4*A*). The analysis of the amino acid profile of SMM- and AOA-treated cells confirmed the efficiency of the two inhibitors. As expected, SMM caused a sharp drop of Leu

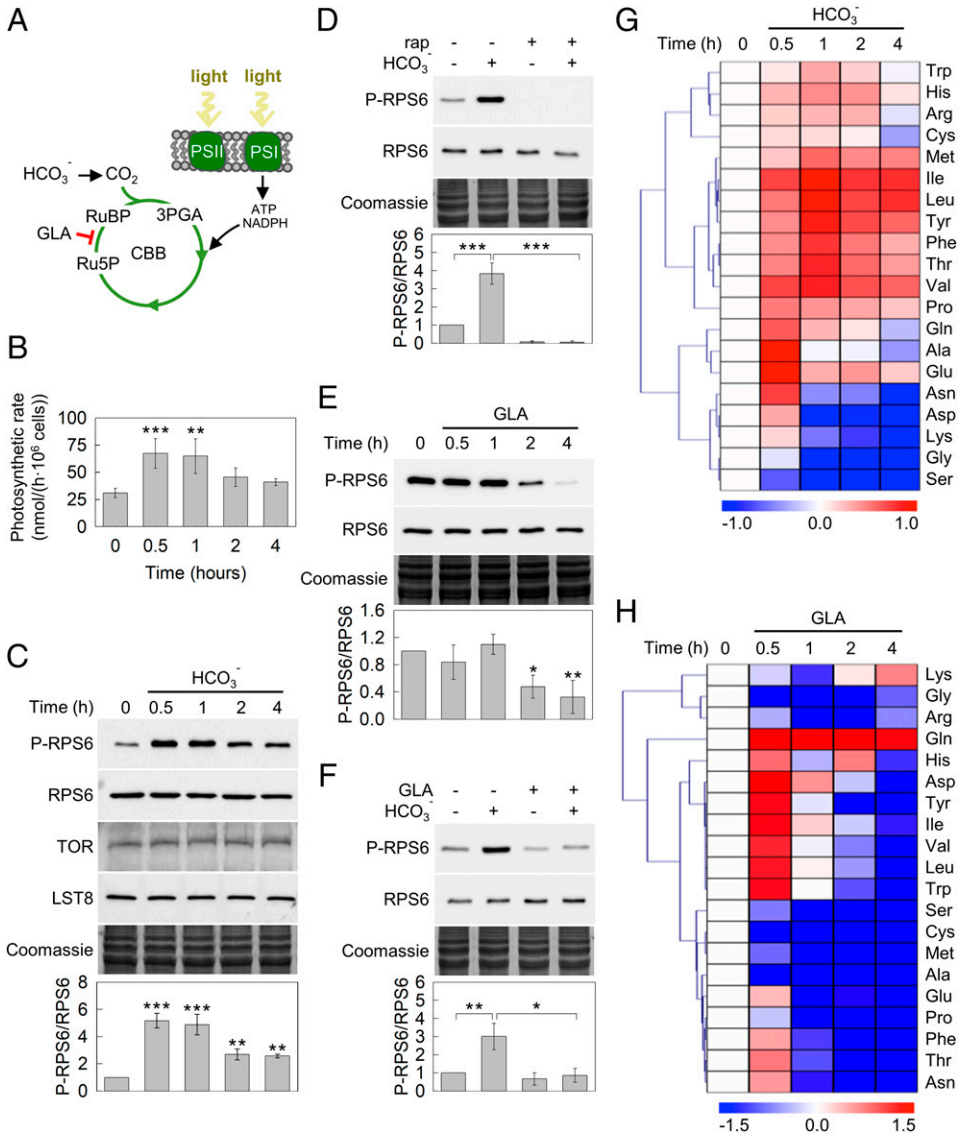

Fig. 2. CO_2 fixation activates TOR signaling in *Chlamydomonas*. (*A*) Schematic representation of photosynthesis and CO_2 fixation. The incorporation of HCO_3^- to the CBB cycle and the inhibitory effect of GLA are indicated. (*B*) Photosynthetic rate of *Chlamydomonas* cells growing in the presence of 10 mM HCO_3^- (0, 0.5, 1, 2, and 4 h) in HSM. Three biological replicates were analyzed for each time point. (*C*) Immunoblot analysis of P-RPS6, RPS6, TOR, and LST8 of *Chlamydomonas* cells grown as described in *B*. (*D*) Western blot analysis of P-RPS6 and RPS6 in *Chlamydomonas* cells treated (+) or not (−) with 1 μM rap for 2 h and then 10 mM HCO_3^- for 0.5 h. (*E*) Western blot analysis of P-RPS6 and RPS6 of *Chlamydomonas* cells treated with 10 mM GLA for 0, 0.5, 1, 2, and 4 h. (*F*) Western blot analysis of P-RPS6 and RPS6 in *Chlamydomonas* cells treated (+) or not (−) with 10 mM GLA for 2 h and then 10 mM HCO_3^- for 0.5 h. Coomassie brilliant blue–stained gels were used as protein loading control. For TOR activity determination in *C* to *F*, the P-RPS6/RPS6 ratio was calculated from three biological replicates (a.u., arbitrary units). Untreated cells were used as control. Error bars represent SD of the mean values. Asterisks in *B*, *C*, and *E* represent significant differences according to one-way ANOVA and Bonferroni's test: $*P < 0.05$, $**P < 0.01$, and $***P < 0.001$. Asterisks in *D* and *F* represent significant differences according to two-tailed Student's *t* test: $**P < 0.01$ and $***P < 0.001$. (*G*, *H*) Hierarchical clustering analysis showing the relative abundance of each amino acid over the time course in HCO_3^- (*G*) or GLA (*H*) treatment after normalization to untreated (0 h) sample using log2 transformation. Four biological replicates were analyzed for each treatment.

and Val, whereas AOA led to a pronounced decrease of Ala (Fig. 4*B*). However, the down-regulation of Leu, Val, and Ala synthesis by SMM and AOA also resulted in a strong increase of some amino acids, probably because of the redirection of fixed carbon to the synthesis of other amino acids and/or the activity of transaminases. Indeed, SMM boosted the level of Gln, Glu, and Ala among other amino acids while AOA markedly raised Leu, Val, Gln, Glu, Asp, Asn, and Pro abundance (Fig. 4*B*). We next analyzed the effect of SMM and AOA on TOR activity. Notably, TOR activity was up-regulated in cells treated with these inhibitors, indicating that TOR responds to changes in amino acid abundance (Fig. 4*C*). Moreover, we found that the inhibition of carbon fixation by GLA fully prevented the up-regulation of TOR induced by SMM and AOA (Fig. 4*D*). Thus, our results revealed that carbon fixation is the primary regulator of TOR activity in SMM- and AOA-treated cells and demonstrated a direct link between the abundance of intracellular amino acids and TOR in *Chlamydomonas*.

Starch Deficiency Up-Regulates TOR Activity. Starch biosynthesis is an essential outlet of photosynthetic electron transport. In *Chlamydomonas*, it has been shown that the disruption of starch synthesis results in a pronounced drop in photosynthetic capacity and the redirection of photosynthetically fixed carbon

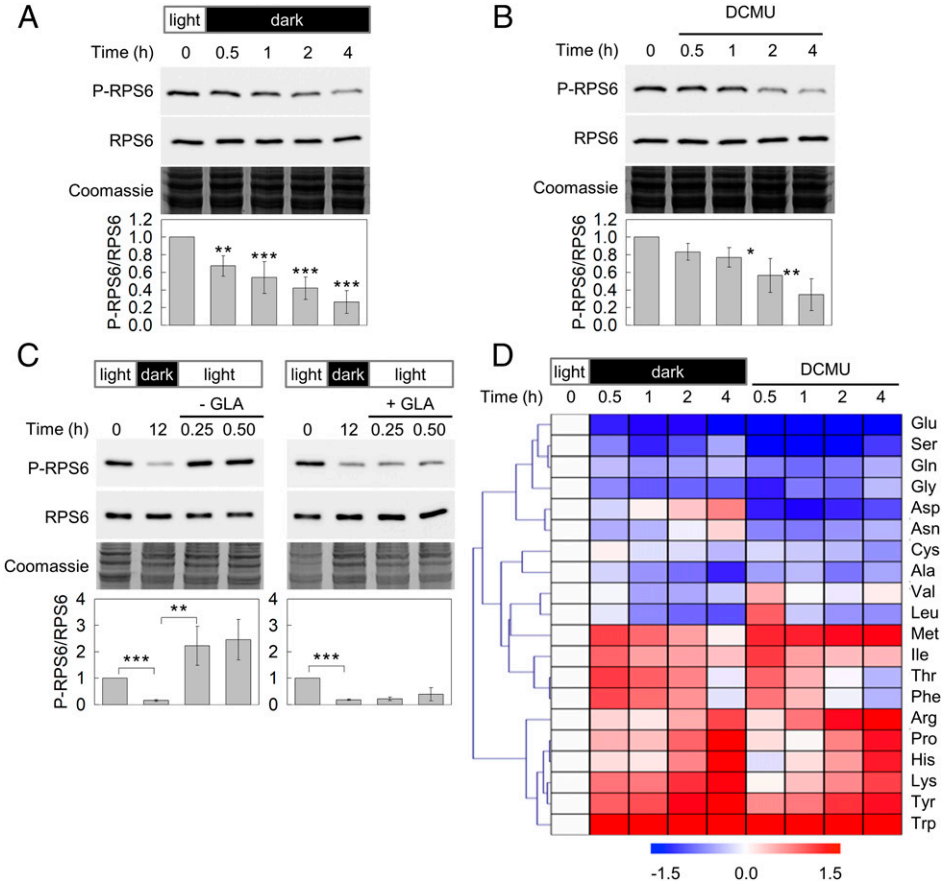

Fig. 3. Inhibition of photosynthesis down-regulates TOR activity in *Chlamydomonas*. (*A*) Western blot analysis of P-RPS6 and RPS6 in wild-type *Chlamydomonas* cells in HSM transferred from standard light illumination (0 h) to darkness for 0.5, 1, 2, and 4 h. (*B*) Western blot analysis of P-RPS6 and RPS6 in *Chlamydomonas* cells grown in HSM and treated with 20 μM DCMU for 0, 0.5, 1, 2, and 4 h. TOR activity in *A* and *B* was determined as described in Fig. 1*B*. (*C*) Hierarchical clustering analysis showing the relative abundance of each amino acid over the time course in cells shifted from light to dark or treated with 20 μM DCMU after normalization to 0 h sample using log2 transformation. Four biological replicates were analyzed for each treatment in *B* and *C*. (*D*) Cells growing in the light were shifted to dark for 12 h and then reilluminated for 15 or 30 min. Prior to the dark-to-light transition, cells were treated with 10 mM GLA for 30 min. P-RPS6 and RPS6 were detected by Western blot in these conditions. Coomassie brilliant blue–stained gels were used as protein loading control. For TOR activity quantification in *A*, *B*, and *D*, the P-RPS6/RPS6 ratio was calculated from five, four, and three biological replicates, respectively. Untreated cells were used as control. Error bars represent SD of the mean values. Asterisks in *A* and *B* represent significant differences according to one-way ANOVA and Bonferroni's test: $*P < 0.05$, $**P < 0.01$, and $***P < 0.001$. Asterisks in *C* represent significant differences according to two-tailed Student's *t* test: $**P < 0.01$ and $***P < 0.001$.

under autotrophic conditions (41). Thus, to further explore the connection between TOR and carbon fixation in *Chlamydomonas*, we analyzed TOR activity in the *sta6* mutant, which is unable to synthesize starch because of the lack of the enzyme ADP glucose pyrophosphorylase (42). Since the *sta6* mutant was generated in the cell wall–deficient *cw15* background (42), first of all we confirmed that *cw15* and wild-type cells display the same basal TOR activity in our experimental setup (*SI Appendix*, Fig. S3*A*). Actually, we also determined the amino acid profile in both strains, and no significant differences were detected for any amino acid (*SI Appendix*, Fig. S3*B*). Remarkably, the analysis of RPS6 phosphorylation in *sta6* cells revealed a much higher TOR activity in this mutant compared to the *cw15* strain (Fig. 5*A*), indicating that the inability to synthesize starch up-regulates TOR. To exclude that the up-regulation of TOR activity in *sta6* cells might be related to additional mutations reported in this strain (43), we also monitored RPS6 phosphorylation in a *sta6*-rescued strain (44). As anticipated, the complemented *sta6* strain exhibited the same level of RPS6 phosphorylation as *cw15* cells (*SI Appendix*, Fig. S4*A*).

Given the tight connection found between TOR activity and the amino acid content in *Chlamydomonas*, we determined the amino acid abundance of *sta6* cells under autotrophic growth. The total amino acid content was around 60% higher in the *sta6* mutant (*SI Appendix*, Fig. S4*B*). All amino acids other than Ile, Tyr, Thr, Trp, and Phe were up-regulated in *sta6* cells (Fig. 5*B*), although the most remarkable increase was detected in the Gln content, which was eight times higher (*SI Appendix*, Fig. S4*C*). To further investigate the misregulation of TOR in the starch-deficient *sta6* mutant, we determined TOR activity and amino acid abundance in this strain under conditions that either increase or diminish the activity of TOR. On the one hand, addition of HCO_3^- to *cw15* and *sta6* cells stimulated TOR activity in both strains, although to a different range. Like in wild-type cells (Fig. 2*B*), HCO_3^- led to a sevenfold raise of TOR activity in *cw15* cells, whereas this increase was less pronounced in the *sta6* mutant (Fig. 5*C*). The effect of HCO_3^- in the amino acid content of *cw15* and *sta6* cells was similar, but some amino acids like Gln did not increase in the *sta6* mutant (Fig. 5*B*), probably because of the massive concentration of this amino acid before HCO_3^- addition (*SI Appendix*, Fig. S4*C*). On the other hand, inhibition of CO_2 fixation or photosynthesis down-regulated TOR activity in *sta6* cells to levels comparable to the ones detected in *cw15* cells despite the much higher

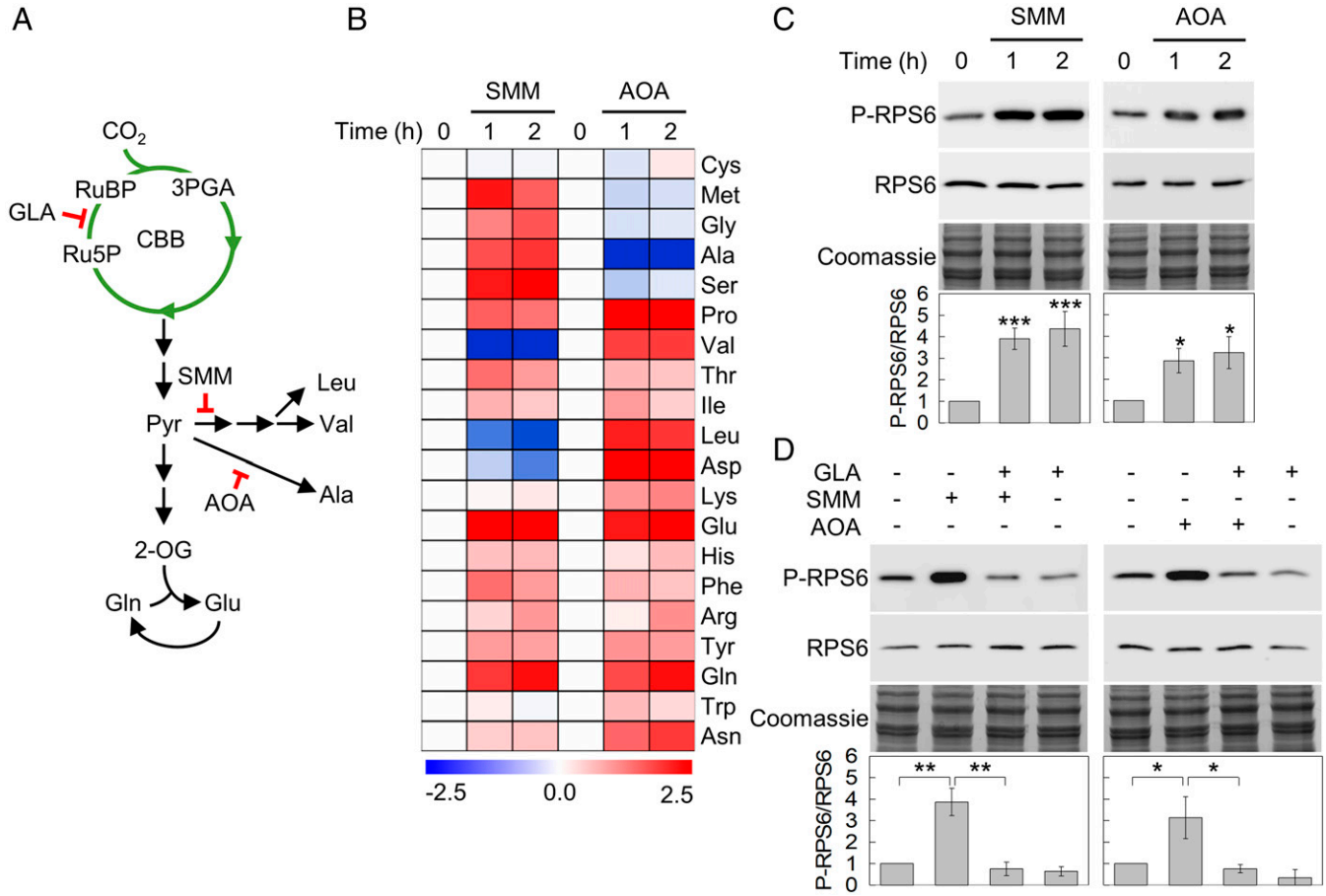

Fig. 4. TOR activity responds to the intracellular abundance of amino acids. (*A*) Schematic representation of CO_2 fixation and the metabolic pathways for the synthesis of Val, Leu, Ala, Glu, and Gln. The inhibitory effect of GLA, SMM, and AOA is indicated. (*B*) Heat map showing the relative abundance of each amino acid over the time course in SMM or AOA treatment after normalization to untreated (0 h) sample using log2 transformation. (*C*) Western blot analysis of P-RPS6 and RPS6 in *Chlamydomonas* cells grown in HSM and treated with 5 μM SMM or 1 mM AOA for 1 and 2 h, respectively. (*D*) Western blot analysis of P-RPS6 and RPS6 in *Chlamydomonas* cells treated (+) or not (−) with 10 mM GLA for 2 h and 5 μM SMM or 1 mM AOA for 1 h. Coomassie brilliant blue–stained gels were used as protein loading control. For TOR activity determination in *C* and *D*, the P-RPS6/RPS6 ratio was calculated from three biological replicates (a.u.). Untreated cells were used as control. Error bars represent SD of the mean values. Asterisks in *C* and *D* represent significant differences according to Bonferroni's test and one-way ANOVA, respectively: $*P < 0.05$, $**P < 0.01$, and $***P < 0.001$.

TOR activity inherent to the starchless mutant (Fig. 5 *D–F*). The analysis of the amino acid content under these conditions revealed similar effects for most amino acids except Ile, Tyr, Thr, Trp, and Phe, which were less abundant in the *sta6* mutant and markedly increased in response to the inhibition of CO_2 fixation or photosynthesis (Fig. 5*B*). Taken together, these results suggested that the higher TOR activity of the *sta6* mutant might be due to the elevated concentration of key amino acids such as Gln, which activates TOR signaling in yeast and mammalian cells (4).

Discussion

The CBB cycle catalyzes the incorporation of inorganic CO_2 into organic molecules, an essential process performed by photosynthetic organisms that keeps life on Earth. In this study, we found that CO_2 fixation promotes the activity of the cell growth master regulator TOR in the green alga *Chlamydomonas*. The TOR pathway integrates different nutrient signals including the availability of organic carbon compounds like glucose. In nonphotosynthetic eukaryotes, glucose is the major carbon source and TOR perceives glucose deficiency through the AMPK/Snf1 kinase (4). In plants, it has been shown that exogenous glucose taken up by root glucose transporters activates TOR kinase activity (12). Glucose-TOR signaling seems to be a main channel for the regulation of central metabolism in plants, as profound transcriptional reprograming takes place in metabolic networks upon glucose stimulation of TOR (12). Chemical targeting of mitochondria demonstrated that glucose-mediated activation of plant TOR depends on mitochondrial electron transport chain and oxidative phosphorylation (12).

In the absence of exogenous carbon supply, CO_2 fixation provides carbon skeletons for all reactions in photosynthetic cells. In order to sustain cell growth, a significant portion of fixed carbon is invested in the synthesis of amino acids (34). In close agreement, we found that HCO_3^- addition to *Chlamydomonas* cells quickly increased the level of all amino acids except Gly and Ser, which are likely down-regulated due to a decrease of rubisco oxygenase activity and photorespiration (Fig. 2*G*). Conversely, inhibition of CO_2 fixation resulted in a sharp drop of most amino acids (Fig. 2*H*), corroborating the role of fixed carbon in the synthesis of amino acids. Our results also demonstrated that carbon fixation regulates TOR activity in *Chlamydomonas*. Stimulation of CO_2 fixation with HCO_3^- boosted TOR activity, whereas inhibition of this fundamental process led to a strong decline of TOR activity (Fig. 2). Moreover, the amino acid profile of *Chlamydomonas* cells subjected to different carbon sources or treated with inhibitors of carbon fixation,

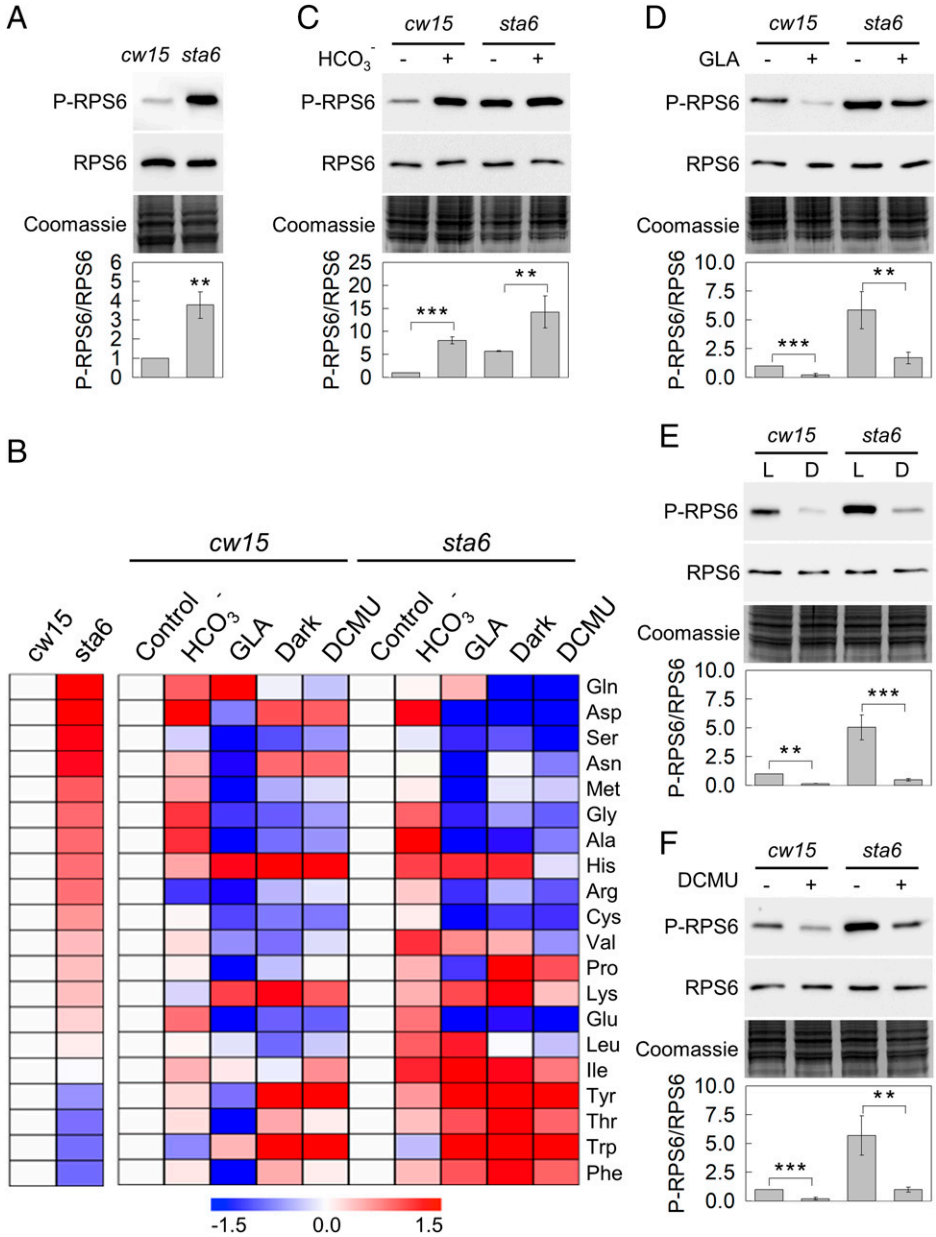

Fig. 5. TOR activity is up-regulated in the *Chlamydomonas* starchless mutant *sta6*. (*A*) Western blot analysis of P-RPS6 and RPS6 in *cw15* and *sta6 Chlamydomonas* strains growing exponentially in HSM. Three biological replicates were analyzed in both strains. (*B*) Heat map showing the relative abundance of each amino acid in *cw15* and *sta6* cells under the following conditions: control, HCO_3^- (10 mM, 30 min), GLA (10 mM, 2 h), dark (2 h), and DCMU μM, 2 h). On the *Left*, each amino acid level is shown normalized to *cw15* cells. On the *Right*, each amino acid level is displayed under the different treatments normalized to untreated cells in both strains. The normalization was calculated using log2 transformation. Four biological replicates were analyzed for each treatment in both strains. (*C*–*F*) Western blot analysis of P-RPS6 and RPS6 in *cw15* and *sta6* cells grown in HSM and subjected to the different conditions shown in *B*. L and D in *E* refer to light and dark, respectively. Coomassie brilliant blue–stained gels were used as protein loading control in all cases. For TOR activity measurements, the P-RPS6/RPS6 ratio was calculated from three biological replicates. Untreated cells were used as control. Error bars represent SD of the mean values. Asterisks in *A* and *C* to *F* represent significant differenced according to two-tailed Student's *t* test: $^{**}P < 0.01$ and $^{***}P < 0.001$.

photosynthesis, or amino acid synthesis uncovered a close link between the kinase activity of TOR and the abundance of Ala, Glu, Gln, Leu, and Val (Fig. 6). Thus, in close agreement with the established and evolutionarily conserved role of amino acids as TOR regulators (4), our study strongly suggests that the modulation of TOR activity by fixed carbon in *Chlamydomonas* is ultimately governed by the intracellular abundance of a subset of key amino acids (Fig. 6).

In yeast and mammalian cells, Leu and Gln regulate TORC1 signaling via the RAG family of small GTPases (4). Recent studies performed in *Arabidopsis* indicated that amino acids are also key upstream signals for plant TOR activation. Accumulation of branched chained amino acids, particularly Val, in a mutant defective in Leu biosynthesis leads to up-regulation of TOR activity (13). Moreover, the same study showed that exogenous feeding of plants with Val, Leu, and Ile stimulated TOR activity (13). Similarly, incubation of *Arabidopsis* leaf discs in Ile or Gln up-regulated TOR activity (15). An in-depth analysis of TOR regulation by nitrogen and amino acids in *Arabidopsis* revealed an efficient activation of TOR by exogenously supplied amino acids, although with different capacities (17). A group of amino acids composed by Ala, Gln, Gly, Cys, Ser, Glu, Asp, and Leu exhibited

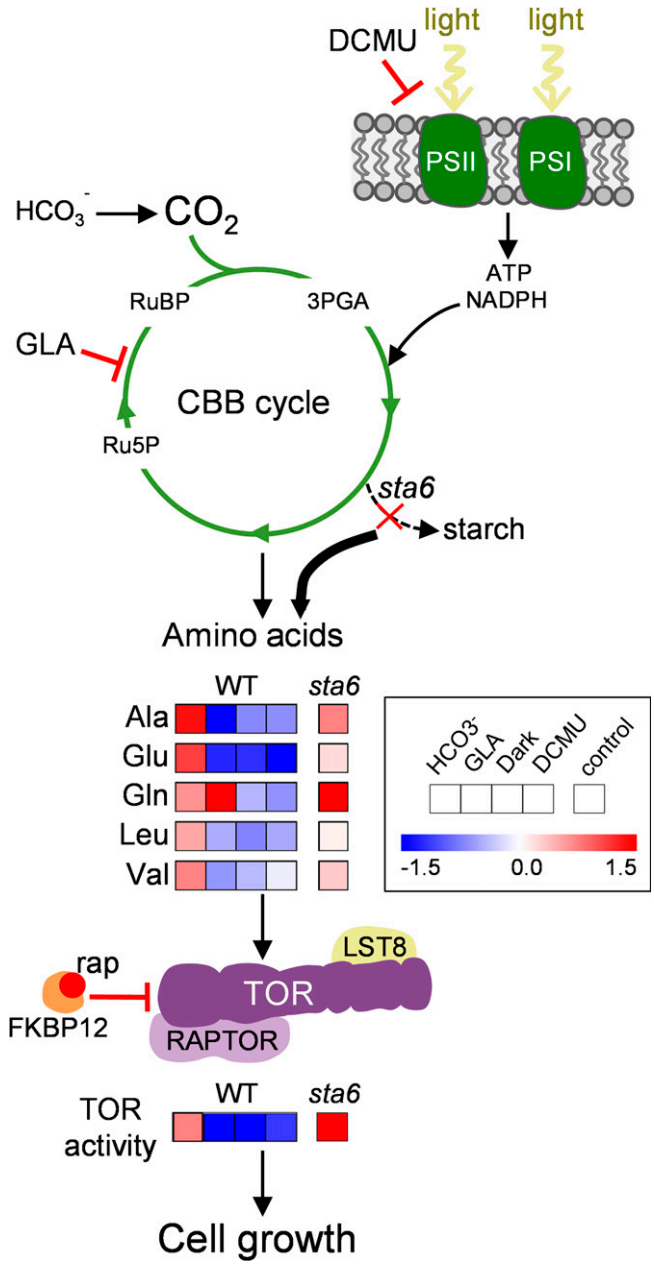

Fig. 6. Proposed model for the regulation of TOR activity by inorganic carbon in *Chlamydomonas*. The CBB cycle catalyzes the incorporation of inorganic CO_2 into organic molecules such as amino acids and starch, a main carbon sink in photosynthetic cells. Photosynthesis provides ATP and NADPH to fuel chemical reactions from the CBB cycle. The availability of fixed carbon modulates the endogenous level of Ala, Glu, Gln, Leu, and Val, increasing with HCO_3^- and decreasing upon inhibition of CO_2 fixation (GLA) or photosynthesis (DCMU, dark). These amino acids regulate TOR activity, which couples carbon sufficiency to cell growth. The inability of the *sta6* mutant to synthesize starch redirects part of the fixed carbon to the synthesis of amino acids, particularly Gln, leading to a massive increase of TOR activity. Heat maps show the relative levels of amino acids and TOR activity in *Chlamydomonas* cells under the conditions indicated in Figs. 2, 3, and 5. Inhibitors of CO_2 fixation (GLA), photosynthesis (DCMU), and TOR (rap) are indicated.

high potency for *Arabidopsis* TOR activation, while other amino acids had little or no regulatory effect on TOR activity (17).

Despite the evolutionary distance between plants and algae, our study in *Chlamydomonas* also connected TOR activity regulation to a similar set of amino acids. Fluctuations in carbon availability resulted in profound changes in TOR activity and the endogenous level of Ala, Glu, Gln, Leu, and Val, reinforcing the tight relationship among carbon fixation, amino acids, and TOR in photosynthetic organisms (Fig. 6). Furthermore, experiments performed with amino acid synthesis inhibitors demonstrated a direct connection between intracellular amino acid abundance and TOR. Blocking the synthesis of Ala or the branched chain amino acids Val and Leu resulted in a marked increase of other central amino acids and the up-regulation of TOR activity (Fig. 4). The amino acids identified in *Chlamydomonas* as potential TOR regulators are generated from the central carbon-skeleton donors pyruvate (Ala, Leu, and Val) and α-ketoglutarate (Glu and Gln) (*SI Appendix*, Fig. S5). Remarkably, a similar conclusion was reached in *Arabidopsis* since addition of amino acids derived from pyruvate or the nitrogen-assimilation pathway exhibited the highest TOR-activating capacity (17). The same study also concluded that external supply of amino acids originating from glycolate (Gly, Ser) and sulfur-assimilation (Cys) pathways led to high activation of TOR (17). However, the endogenous levels of Gly, Ser, and Cys followed an opposite trend to TOR activation in *Chlamydomonas* (*SI Appendix*, Fig. S5), precluding these amino acids as potential regulators of TOR activity in response to carbon availability.

The molecular mechanisms by which TOR perceives amino acids have been reported only in yeast and mammals. Yeast TORC1 seems to sense Leu availability through the Leu–transfer RNA synthetase (45). In mammalian cells, the cytosolic proteins SESTRIN2 and CASTOR1 have been identified respectively as specific sensors of Leu and Arg acting upstream of mTORC1 (5). How mTORC1 perceives Gln is unclear, but it has been reported that activation of mTORC1 by Gln occurs via glutaminolysis (46). Neither orthologs of Leu and Arg sensors nor upstream mTORC1 regulators have been identified in plant and algal genomes, suggesting that the TOR pathway might have experienced specific evolutionary adaptations in the green lineage. Unlike yeast and mammals, algae and plants are autotrophic and can synthesize all amino acids using CO_2 as the sole carbon source. Thus, photosynthetic eukaryotes might have developed unique mechanisms to signal carbon and amino acid sufficiency to the TOR pathway.

The finding that the *Chlamydomonas* starchless mutant *sta6* displays excessive TOR activity provided a further connection of carbon assimilation and amino acids to TOR signaling. Our results indicate that the inability of *sta6* cells to synthesize starch redirects part of the assimilated carbon to the synthesis of amino acids (Fig. 5), as revealed by the higher abundance detected in the *sta6* mutant of most amino acids, notably Gln, which increased eight times. Given the direct link identified in this study between amino acids and TOR (Fig. 4), it is plausible that redirection of fixed carbon to the synthesis of amino acids boosted TOR activity in the *sta6* mutant (Fig. 6). Supporting this conclusion, we found that inhibition of carbon fixation or photosynthesis abolished the hyperactivation of TOR in *sta6* cells (Fig. 5). The TOR pathway has been shown to regulate starch metabolism in plants and algae. Mutations in the *LST8-1* gene or down-regulation of *AtTOR* expression triggers starch accumulation in *Arabidopsis* (47, 48). Similarly, treatment of *Chlamydomonas* or the unicellular red alga *Cyanidioschyzon merolae* with rapamycin increases the starch content (26, 49). However, the impact of starch deficiency on plant TOR signaling has not been explored yet. Our study suggests that starch might regulate cell growth in *Chlamydomonas* since starch deficiency activates TOR, the main growth-promoting pathway in the cell. This hypothesis is in agreement with a previous study in plants showing that starch acts as a major integrator in the regulation of plant growth (50).

In conclusion, we have shown that CO_2 fixation and photosynthesis activate TOR signaling in *Chlamydomonas*, likely

through the synthesis of key amino acids. The regulation of TOR and cell growth by inorganic carbon might have biotechnological implications in algae and plants. Photosynthetic organisms are responsible for converting sunlight and CO_2 into organic matter and are therefore visualized as a resource for the renewable fuel industry and a solution to mitigate the problem of raising concentrations of atmospheric CO_2 (51). Therefore, modulation of TOR activity by inorganic carbon might help to improve biomass productivity in algae and plants, directly influencing agricultural yield or biofuel production.

Materials and Methods

***C. reinhardtii* Strains and Growth Conditions.** *C. reinhardtii* strains used in this study were wild-type 4A+, *cw15*, *sta6*, and complemented *sta6* (termed as C6) and are available as CC-4051, CC-4349, CC-4348, and CC-4567, respectively, from the Chlamydomonas Resource Center (https://www.chlamycollection.org/). *Chlamydomonas* cells were grown under standard illumination (~50 μE m^{-2} s^{-1} from light-emitting diode lamps) in HSM or TAP medium (38) on an orbital shaker (100 rpm) at 25 °C. When required, cells in exponential growth phase (~2×10^6 cells mL^{-1}) were treated with HCO_3^- (Sigma-Aldrich, S5761), GLA (Sigma-Aldrich, G-9376), rapamycin (rap; Cayman Chemical, 53123–88-9), DCMU (Sigma-Aldrich, D7763), SMM (Sigma-Aldrich, 34224), or AOA (Sigma-Aldrich, C-13408) at the indicated concentrations and time. For light-to-dark transition experiments, cells grown in HSM were transferred from standard illumination to complete darkness for the indicated time. Growth rates were estimated during exponential growth phase according to the formula $\mu = \ln(N/N_0)/t$, where N_0 and N represent the cell number at $t = 0$ h and $t = 24$ h, respectively. μ is expressed in h^{-1}. Cell number was determined using a Countess II FL Automated Cell Counter (Invitrogen).

Protein Preparation, Western Blot Assays, and TOR Activity Determination. Protein electrophoresis in denaturing conditions was performed as previously described (25). *Chlamydomonas* cells from liquid cultures were collected by centrifugation (4,000 × *g*, 2 min), washed in lysis buffer [50 mM Tris·HCl (pH 7.5)], and resuspended in a minimal volume of the same buffer. Cells were lysed by two cycles of slow freezing to −80 °C followed by thawing at room temperature. The soluble protein cell extract was separated from the insoluble fraction by centrifugation (15,000 × *g*, 20 min, 4 °C). Proteins were quantified using the Coomassie dye binding method (Bio-Rad, 500–0006) as described by the manufacturer.

For immunoblot analyses, total protein extracts (15 to 40 μg) were subjected to sodium dodecyl sulfate–polyacrylamide gel electrophoresis and then transferred to either polyvinylidene fluoride membrane (Millipore, IPVH00010) previously activated in methanol for P-RPS6 detection or nitrocellulose membrane (Amersham, 10600003) for detection of other proteins. Primary antibodies raised against *Chlamydomonas* P-RPS6 and RPS6 (32), TOR (21), and LST8 (21) proteins and secondary anti-rabbit (Sigma-Aldrich, A6154) were diluted 1:6,000, 1:6,000, 1:1,000, 1:6,000, and 1:10,000, respectively, in phosphate-buffered saline containing 0.1% (vol/vol) Tween-20 (Applichem, A4974) and 5% (wt/vol) milk powder (Applichem, A0830). Proteins were detected with the Luminata Crescendo Millipore immunoblotting detection system (Millipore, WBLUR0500) and visualized using a ChemiDoc Imaging System (Bio-Rad). Coomassie brilliant blue–stained gels were used as protein loading control.

For determination of the phosphorylation status of RPS6, phosphorylated (P-RPS6) and total RPS6 were quantified using the ImageLab software (Bio-Rad), and the P-RPS6/RPS6 ratio was calculated as previously described (32).

Amino Acid Analysis. To determine the amino acid profile, *Chlamydomonas* cells growing exponentially (~2×10^6 cells mL^{-1}) under the indicated treatment were collected by centrifugation (4,000 × *g*, 2 min) and immediately frozen in liquid nitrogen. Cells were then lyophilized and 2 mg of dried weight for each condition were used to extract amino acids. Cells were resuspended with HCl 0.1 N, mixed by vortexing, and then incubated on ice for 1 h. After centrifugation (15,000 × *g*, 15 min) at 4 °C to remove cells debris, the supernatant was transferred to a fresh tube and used to analyze the amino acid content by mass spectrometry (Sciex 6500+ QTRAP hybrid triple quadrupole liquid chromatography with tandem mass spectrometry). Amino acids were quantified using a standard amino acid mixture (Sigma-Aldrich). At least four biological replicates were analyzed for each condition.

Oxygen Evolution Measurement. *Chlamydomonas* cells growing autotrophically in HSM medium were incubated with bicarbonate, DCMU, or GLA for the indicated time, and then 2 mL of cells (~2×10^6 cells mL^{-1}) was used to determine oxygen evolution at 25 °C with continuous stirring in a Clark-type electrode (Chlorolab 2+ System; Hansatech). Photosynthetic rate was calculated as the difference between oxygen production in the light and oxygen consumption in the dark. Oxygen production was analyzed for 5 min at 60 μmol photons m^{-2} s^{-1}. Cells were then exposed to darkness for 5 min to calculate oxygen consumption.

Chlorophyll Fluorescence Measurement. Chlorophyll fluorescence measurements were performed using a DUAL-PAM-100 (Walz). *Chlamydomonas* cells growing autotrophycally in HSM medium were incubated with DCMU or GLA for the indicated time, and then 2 mL of cells (~2×10^6 cells mL^{-1}) was used to determine relative electron transport rate (rETR) and maximum photochemical efficiency (Fv/Fm). Cells were dark adapted for 15 min with constant stirring to obtain the Fv/Fm ratio. Cells were then exposed to 50 μmol photons m^{-2} s^{-1} for 5 min to quantify rETR values.

Statistics. Data from at least three independent experiments were analyzed using SigmaPlot 11 software. Two-tailed Student's *t* tests were used to compare different strains, different growing conditions, and different treatments. One-way ANOVA followed by Bonferroni's post hoc comparisons tests were used to analyze the temporal changes in the different treatments. $P < 0.05$ was taken as the threshold for statistical significance. Single (*), double (**), and triple (***) asterisks indicate a significant difference: $P < 0.05$, $P < 0.01$, and $P < 0.001$, respectively. For amino acid analysis, heat map showing the fold changes were generated using the MeV software. Amino acid correlations were clustered with hierarchical clustering using Pearson correlation for the distance measure and average linkage for the linkage method. A summary of the statistical analysis of experiments shown in main and supplementary figures can be found in *SI Appendix*, Tables S1 and S2, respectively.

Data Availability. All study data are included in the article and/or *SI Appendix*.

ACKNOWLEDGMENTS. This work was supported in part by Ministerio de Ciencia y Tecnología (Grants PGC2018-099048-B-I00 to J.L.C. and PID2019-110080GB-I00 to M.E.P.-P.) and Consejo Superior de Investigaciones Científicas (Grant 202040I006 to M.E.P.-P.). We thank Carlos Parejo for technical assistance with the analysis of amino acid profiles.

1. M. Laplante, D. M. Sabatini, mTOR signaling in growth control and disease. *Cell* **149**, 274–293 (2012).
2. S. Wullschleger, R. Loewith, M. N. Hall, TOR signaling in growth and metabolism. *Cell* **124**, 471–484 (2006).
3. R. Loewith *et al.*, Two TOR complexes, only one of which is rapamycin sensitive, have distinct roles in cell growth control. *Mol. Cell* **10**, 457–468 (2002).
4. A. González, M. N. Hall, Nutrient sensing and TOR signaling in yeast and mammals. *EMBO J.* **36**, 397–408 (2017).
5. R. L. Wolfson, D. M. Sabatini, The dawn of the age of amino acid sensors for the mTORC1 pathway. *Cell Metab.* **26**, 301–309 (2017).
6. M. Binda *et al.*, The Vam6 GEF controls TORC1 by activating the EGO complex. *Mol. Cell* **35**, 563–573 (2009).
7. L. Fu, P. Wang, Y. Xiong, Target of rapamycin signaling in plant stress responses. *Plant Physiol.* **182**, 1613–1623 (2020).
8. C. Ingargiola, G. Turqueto Duarte, C. Robaglia, A. S. Leprince, C. Meyer, The plant target of rapamycin: A conduc TOR of nutrition and metabolism in photosynthetic organisms. *Genes (Basel)* **11**, 1285 (2020).
9. Y. Mugume, Z. Kazibwe, D. C. Bassham, Target of rapamycin in control of autophagy: Puppet master and signal integrator. *Int. J. Mol. Sci.* **21**, 8259 (2020).
10. M. Schepetilnikov *et al.*, TOR and S6K1 promote translation reinitiation of uORF-containing mRNAs via phosphorylation of eIF3h. *EMBO J.* **32**, 1087–1102 (2013).
11. P. Wang *et al.*, Reciprocal regulation of the TOR kinase and ABA receptor balances plant growth and stress response. *Mol. Cell* **69**, 100–112.e6 (2018).
12. Y. Xiong *et al.*, Glucose-TOR signalling reprograms the transcriptome and activates meristems. *Nature* **496**, 181–186 (2013).
13. P. Cao *et al.*, Homeostasis of branched-chain amino acids is critical for the activity of TOR signaling in *Arabidopsis*. *eLife* **8**, e50747 (2019).
14. M. Schaufelberger *et al.*, Mutations in the Arabidopsis ROL17/isopropylmalate synthase 1 locus alter amino acid content, modify the TOR network, and suppress the root hair cell development mutant lrx1. *J. Exp. Bot.* **70**, 2313–2323 (2019).
15. B. M. O'Leary, G. G. K. Oh, C. P. Lee, A. H. Millar, Metabolite regulatory interactions control plant respiratory metabolism via target of rapamycin (TOR) kinase activation. *Plant Cell* **32**, 666–682 (2020).

16. D. Deprost *et al.*, The Arabidopsis TOR kinase links plant growth, yield, stress resistance and mRNA translation. *EMBO Rep.* **8**, 864–870 (2007).
17. Y. Liu *et al.*, Diverse nitrogen signals activate convergent ROP2-TOR signaling in Arabidopsis. *Dev. Cell* **56**, 1283–1295.e5 (2021).
18. S. Díaz-Troya, M. E. Pérez-Pérez, F. J. Florencio, J. L. Crespo, The role of TOR in autophagy regulation from yeast to plants and mammals. *Autophagy* **4**, 851–865 (2008).
19. A. Shemi, S. Ben-Dor, A. Vardi, Elucidating the composition and conservation of the autophagy pathway in photosynthetic eukaryotes. *Autophagy* **11**, 701–715 (2015).
20. M. E. Pérez-Pérez, I. Couso, J. L. Crespo, The TOR signaling network in the model unicellular green alga *Chlamydomonas reinhardtii*. *Biomolecules* **7**, 54 (2017).
21. S. Díaz-Troya, F. J. Florencio, J. L. Crespo, Target of rapamycin and LST8 proteins associate with membranes from the endoplasmic reticulum in the unicellular green alga *Chlamydomonas reinhardtii*. *Eukaryot. Cell* **7**, 212–222 (2008).
22. J. L. Crespo, S. Díaz-Troya, F. J. Florencio, Inhibition of target of rapamycin signaling by rapamycin in the unicellular green alga *Chlamydomonas reinhardtii*. *Plant Physiol.* **139**, 1736–1749 (2005).
23. S. Díaz-Troya *et al.*, Inhibition of protein synthesis by TOR inactivation revealed a conserved regulatory mechanism of the BiP chaperone in *Chlamydomonas*. *Plant Physiol.* **157**, 730–741 (2011).
24. S. Imamura *et al.*, Target of rapamycin (TOR) plays a critical role in triacylglycerol accumulation in microalgae. *Plant Mol. Biol.* **89**, 309–318 (2015).
25. M. E. Pérez-Pérez, F. J. Florencio, J. L. Crespo, Inhibition of target of rapamycin signaling and stress activate autophagy in *Chlamydomonas reinhardtii*. *Plant Physiol.* **152**, 1874–1888 (2010).
26. J. Jüppner *et al.*, The target of rapamycin kinase affects biomass accumulation and cell cycle progression by altering carbon/nitrogen balance in synchronized *Chlamydomonas reinhardtii* cells. *Plant J.* **93**, 355–376 (2018).
27. U. Mubeen, J. Jüppner, J. Alpers, D. K. Hincha, P. Giavalisco, Target of rapamycin inhibition in *Chlamydomonas reinhardtii* triggers de novo amino acid synthesis by enhancing nitrogen assimilation. *Plant Cell* **30**, 2240–2254 (2018).
28. V. Roustan, W. Weckwerth, Quantitative phosphoproteomic and system-level analysis of TOR inhibition unravel distinct organellar acclimation in *Chlamydomonas reinhardtii*. *Front. Plant Sci.* **9**, 1590 (2018).
29. E. G. Werth *et al.*, Investigating the effect of target of rapamycin kinase inhibition on the *Chlamydomonas reinhardtii* phosphoproteome: From known homologs to new targets. *New Phytol.* **221**, 247–260 (2019).
30. S. Upadhyaya, S. Agrawal, A. Gorakshakar, B. J. Rao, TOR kinase activity in *Chlamydomonas reinhardtii* is modulated by cellular metabolic states. *FEBS Lett.* **594**, 3122–3141 (2020).
31. I. Couso *et al.*, Synergism between inositol polyphosphates and TOR kinase signaling in nutrient sensing, growth control and lipid metabolism in *Chlamydomonas*. *Plant Cell* **28**, 2026–2042 (2016).
32. I. Couso *et al.*, Phosphorus availability regulates TORC1 signaling via LST8 in *Chlamydomonas*. *Plant Cell* **32**, 69–80 (2020).
33. D. D. Wykoff, A. R. Grossman, D. P. Weeks, H. Usuda, K. Shimogawara, Psr1, a nuclear localized protein that regulates phosphorus metabolism in *Chlamydomonas*. *Proc. Natl. Acad. Sci. U.S.A.* **96**, 15336–15341 (1999).
34. X. Johnson, J. Alric, Central carbon metabolism and electron transport in *Chlamydomonas reinhardtii*: Metabolic constraints for carbon partitioning between oil and starch. *Eukaryot. Cell* **12**, 776–793 (2013).
35. Y. Wang, D. J. Stessman, M. H. Spalding, The CO2 concentrating mechanism and photosynthetic carbon assimilation in limiting CO2: How *Chlamydomonas* works against the gradient. *Plant J.* **82**, 429–448 (2015).
36. G. Amoroso, D. Sultemeyer, C. Thyssen, H. P. Fock, Uptake of HCO3 and CO2 in cells and chloroplasts from the microalgae *Chlamydomonas reinhardtii* and *Dunaliella tertiolecta*. *Plant Physiol.* **116**, 193–201 (1998).
37. S. Takahashi, N. Murata, Interruption of the Calvin cycle inhibits the repair of Photosystem II from photodamage. *Biochim. Biophys. Acta* **1708**, 352–361 (2005).
38. E. H. Harris, *The Chlamydomonas Sourcebook*, (Academic Press, San Diego, 2009).
39. M. E. Hartnett, J. R. Newcomb, R. C. Hodson, Mutations in *Chlamydomonas reinhardtii* conferring resistance to the herbicide sulfometuron methyl. *Plant Physiol.* **85**, 898–901 (1987).
40. J. V. Moroney, B. J. Wilson, N. E. Tolbert, Glycolate metabolism and excretion in *Chlamydomonas reinhardtii*. *Plant Physiol.* **82**, 821–826 (1986).
41. S. Saroussi *et al.*, Alternative outlets for sustaining photosynthetic electron transport during dark-to-light transitions. *Proc. Natl. Acad. Sci. U.S.A.* **116**, 11518–11527 (2019).
42. C. Zabawinski *et al.*, Starchless mutants of *Chlamydomonas reinhardtii* lack the small subunit of a heterotetrameric ADP-glucose pyrophosphorylase. *J. Bacteriol.* **183**, 1069–1077 (2001).
43. I. K. Blaby *et al.*, Systems-level analysis of nitrogen starvation-induced modifications of carbon metabolism in a *Chlamydomonas reinhardtii* starchless mutant. *Plant Cell* **25**, 4305–4323 (2013).
44. Y. Li *et al.*, *Chlamydomonas* starchless mutant defective in ADP-glucose pyrophosphorylase hyper-accumulates triacylglycerol. *Metab. Eng.* **12**, 387–391 (2010).
45. G. Bonfils *et al.*, Leucyl-tRNA synthetase controls TORC1 via the EGO complex. *Mol. Cell* **46**, 105–110 (2012).
46. R. V. Durán *et al.*, Glutaminolysis activates Rag-mTORC1 signaling. *Mol. Cell* **47**, 349–358 (2012).
47. C. Caldana *et al.*, Systemic analysis of inducible target of rapamycin mutants reveal a general metabolic switch controlling growth in *Arabidopsis thaliana*. *Plant J.* **73**, 897–909 (2013).
48. M. Moreau *et al.*, Mutations in the *Arabidopsis* homolog of LST8/GβL, a partner of the target of Rapamycin kinase, impair plant growth, flowering, and metabolic adaptation to long days. *Plant Cell* **24**, 463–481 (2012).
49. I. Pancha *et al.*, Target of rapamycin-signaling modulates starch accumulation via glycogenin phosphorylation status in the unicellular red alga *Cyanidioschyzon merolae*. *Plant J.* **97**, 485–499 (2019).
50. R. Sulpice *et al.*, Starch as a major integrator in the regulation of plant growth. *Proc. Natl. Acad. Sci. U.S.A.* **106**, 10348–10353 (2009).
51. S. S. Merchant, J. Kropat, B. Liu, J. Shaw, J. Warakanont, TAG, you're it! *Chlamydomonas* as a reference organism for understanding algal triacylglycerol accumulation. *Curr. Opin. Biotechnol.* **23**, 352–363 (2012).